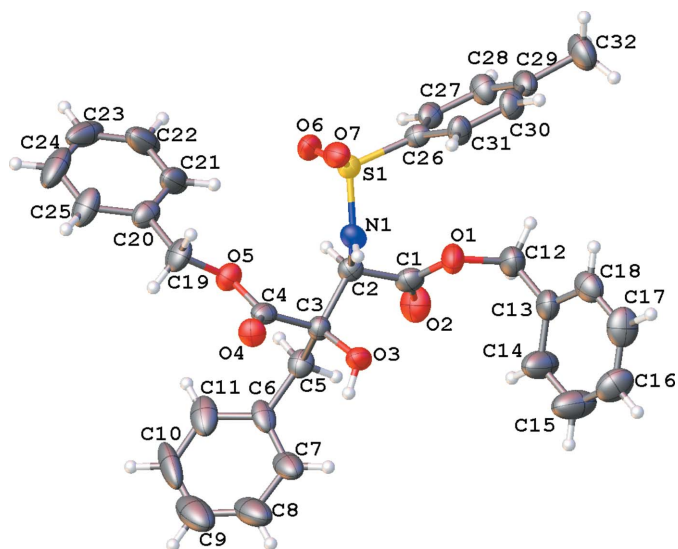
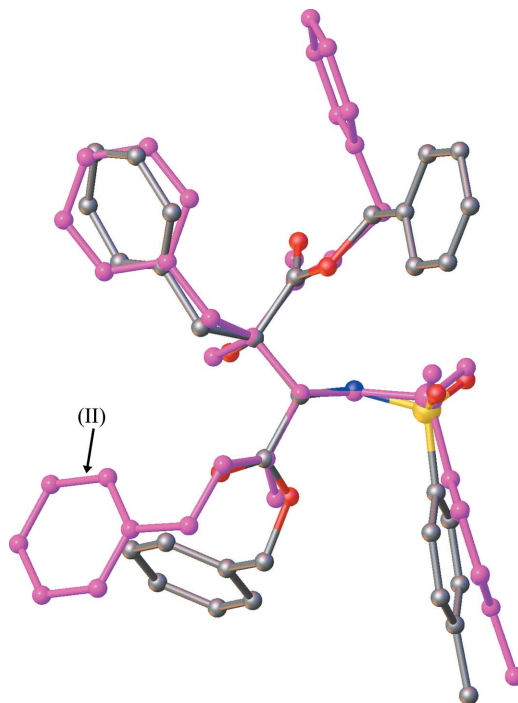


**Figure 1**  
The asymmetric unit of polymorph (I), with displacement ellipsoids for the non-H atoms drawn at the 50% probability level.



**Figure 2**  
The asymmetric unit of polymorph (II), with displacement ellipsoids for the non-H atoms drawn at the 50% probability level. One H atom on each of C12 and C32 is occluded by its parent atom.

Figs. 1 and 2 present atomic displacement representations of the molecular structures of polymorphs (I) and (II), both in the arbitrarily chosen (2*R*,3*R*) configuration. The molecule is an analogue of *L*- $\beta$ -threo-benzyl-Asp-OH with two benzyl esters and a tosyl moiety acting as protecting groups for the carboxylate and amine functions of this amino acid. In order to describe the conformational orientation of the four aromatic rings present in the molecule, we consider ring 1 (C6–C11) from the  $\beta$ -benzyl chain, rings 2 (C13–C18) and 3 (C20–C25) from the two ester functions of the  $\alpha$  and  $\gamma$  carboxylate groups, and ring 4 (C26–C31) from the tosyl moiety protecting the  $\alpha$ -amino group. In polymorph (I), rings 3 and 4 are nearly coplanar, with a dihedral angle of 5.93 (13) $^\circ$ ; for (II), the dihedral angle between these two rings is 42.3 (3) $^\circ$ .

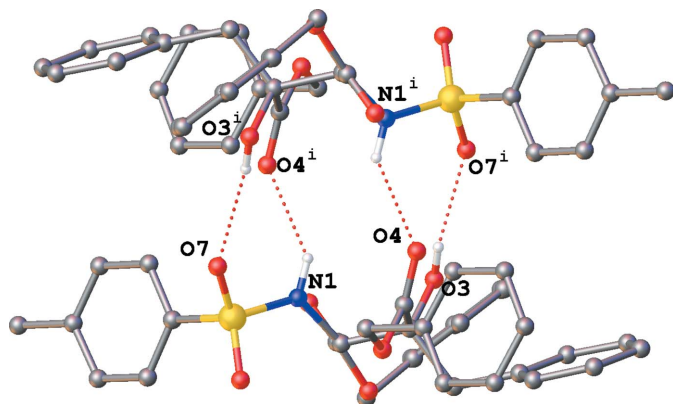


**Figure 3**  
A superposition of the molecular structures of polymorphs (I) and (II) based on the overlapping of the three central atoms (N1, C2 and C3). In the electronic version of the paper, polymorph (II) has been coloured in magenta to highlight differences between its conformation and that of polymorph (I).

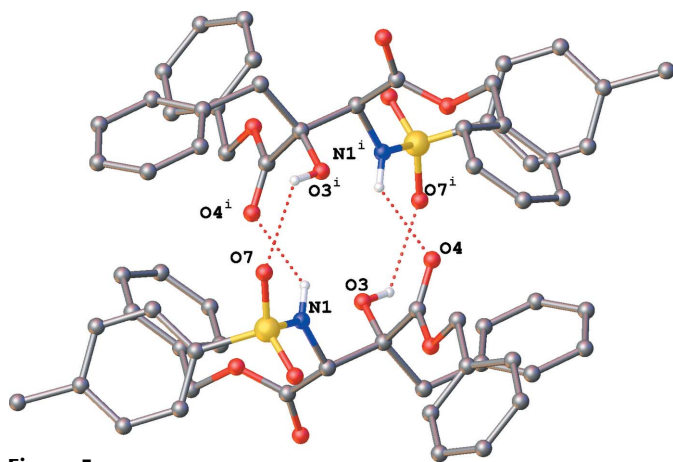
An examination of the mutual orientation of rings 1 and 2 reveals a larger deviation in (II) with dihedral angles of 41.1 (4) $^\circ$  for (II) and 24.01 (15) $^\circ$  for (I).

Fig. 3 shows a superposition of the two (2*R*,3*R*) enantiomers as calculated by *OLEX2* (Dolomanov *et al.*, 2009) based on the overlapping of the three central atoms (N1, C2 and C3). It is acknowledged that this is not the ‘best’ superposition, which would take into account all non-H atoms giving a root-mean-square deviation of 1.743 Å. This figure highlights also that the main difference between the conformations of the two polymorphs lies in the orientation of aromatic rings 2 and 3. This is illustrated by the C4–O5–C19–C20 and N1–C2–C1–O1 torsion angles taken on the same enantiomers of both polymorphs (I) and (II), having values of 84.8 (2) and 178.1 (4) $^\circ$ , and 169.70 (18) and 1.5 (6) $^\circ$ , respectively. For the two other aromatic rings, *viz.* 1 and 4, the values of the C2–C3–C5–C6 and C26–S1–N1–C2 torsion angles are relatively similar at 177.4 (2) and 172.0 (5) $^\circ$  and 88.66 (19) and 81.0 (4) $^\circ$ , respectively. In both polymorphs, the S1–N1 $\cdots$ H1–C2 pseudo-torsion angle [157.7 $^\circ$  for (I) and 153.4 $^\circ$  for (II)] implies a slight pyramidalization of the sulfonamide moiety.

Both polymorphs present the same hydrogen-bond pattern. They are composed of two intermolecular ( $\cdots$ O4–C3–O3–H3 $\cdots$ O7–S1–N1–H1 $\cdots$ ) rings forming the centrosymmetric dimer. This  $R_2^2(9)$  hydrogen-bonding pattern associated with the different conformations described above leads to a dimer that looks like a ‘staircase step’ for (I) and a ‘four-blade double helix’ for (II) (Figs. 4 and 5, and Tables 1 and 2). The hydrogen-bond interactions in both polymorphs are not



**Figure 4**  
The hydrogen-bonded dimer in polymorph (I) of the title compound. Hydrogen bonds are shown as dotted lines and H atoms not involved in hydrogen bonding have been omitted for clarity. Selected atoms of molecules present in the asymmetric unit are labelled to illustrate intermolecular N1–H···O4 and O3–H···O7 hydrogen bonds defining an  $R_2^2(9)$  hydrogen-bonding motif. [Symmetry code: (i)  $-x, -y + 2, -z$ .]



**Figure 5**  
The hydrogen-bonded dimer in polymorph (II) of the title compound. Hydrogen bonds are shown as dotted lines and H atoms not involved in hydrogen bonding have been omitted for clarity. Selected atoms of molecules present in the asymmetric unit are labelled to illustrate intermolecular N1–H···O4 and O3–H···O7 hydrogen bonds defining an  $R_2^2(9)$  hydrogen-bonding motif. [Symmetry code: (i)  $-x + 1, -y, -z + 1$ .]

particularly strong. Although the H···O distances range from 2.17 to 2.30 Å, being well below the sum of the van der Waals radii of H and O, the  $D-H\cdots O$  angles are in the range 127–169°, where the hydrogen-bond interactions in (I) are stronger than in (II). A dimer association formed by two pTos–(NH)–C–(COH)–(C=O)– moieties (pTos is *p*-tosyl or 4-methylbenzenesulfonyl) is absent in the Cambridge Structural Database (CSD, Version 5.32; Allen, 2002). Only three structures present this moiety [DAZQAX (Streuff *et al.*, 2005), PAQZIR (Zhao *et al.*, 2005) and QEJBIR (Streuff *et al.*, 2006)] and dimer association takes place only for PAQZIR, but in a different way, and moreover the latter structure is not an amino acid analogue.

In order to understand semi-quantitatively the apparently easier formation of (I) with respect to (II), we have compared intermolecular energies of (I) and (II) calculated using the

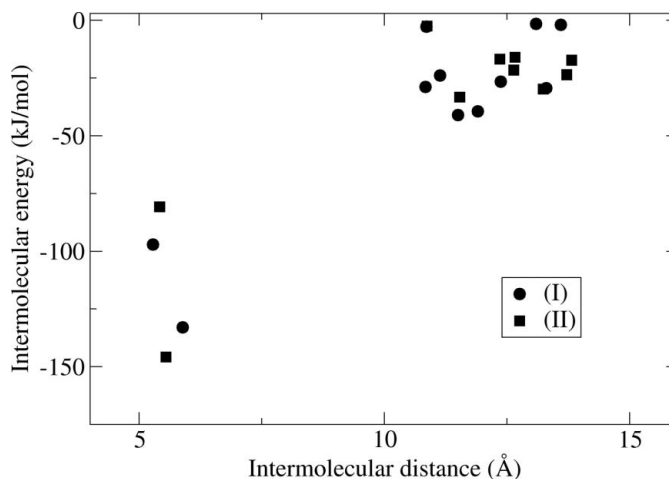


**Figure 6**  
A potential energy plot with respect to the distance between the centre of gravity of the central and surrounding molecules.

UNI potential developed by Gavezzotti (1994) and Gavezzotti & Filippini (1994) and implemented in *Mercury* (Macrae *et al.*, 2006). Hydrogen distance normalization was used. Fig. 6 shows the distance–energy plot for (I) and (II), where the distance is between the centres of gravity of the central and surrounding molecules. The dominating cohesive force comes in both cases from the hydrogen-bonded dimer association and the interaction with one other molecule at an even shorter distance than the dimer pairs but at less negative interaction energy. Despite the overall similarity of the dispersion of the data points, *i.e.* the clustering in two groups, the data points of the two sets show only marginal correlation, proving that the packings, and thus the structures, are far from identical. This finding is reinforced by the calculation of the powder similarity index (PSI) of (I) and (II), using *Mercury*, which significantly differs from 1.0 (0.956), proving the absence of a strong correlation between the packings. Packings which are similar generally give PSIs between 0.98 and 1.00, and lower values are a strong signature of the dissimilarity of the crystal packings. This is supported by the packing analysis of Chisholm & Motherwell (2005) with default parameters; this gives only one molecule in common, indicating that the packings are in fact very dissimilar. The packing energies – which are not identical to lattice energies but should nevertheless give some indications about the relative strengths – calculated for 200 interactions are  $-270.54$  and  $-261.74$  kJ mol $^{-1}$  for (I) and (II), respectively. This explains qualitatively the relative abundance of (I) with respect to (II).

Polymorphic  $P\bar{1}$  and  $P2_1/c$  pairs are not uncommon for organic structures. Out of 1420  $P2_1/c$  organic polymorphic individuals ( $R < 0.10$ ; no disordered structures, duplicates with the same space group removed) and 718  $P\bar{1}$  individuals, 307 polymorphic pairs are found in the CSD (Version 5.32; Allen, 2002).

In summary, dibenzyl 2-benzyl-2-hydroxy-3-(4-methylphenylsulfonamido)succinate crystallizes as two racemic concomitant polymorphs, (I) and (II), of which (I) is much more abundant than (II). The striking feature of the structure

of both polymorphs is the dimer association of the different enantiomers but, owing to the different orientation of two of the substituent groups, the crystal packing differs significantly.

## Experimental

The title compound was recrystallized from a mixture of ethyl acetate and cyclohexane at ambient temperature, yielding colourless crystals in the form of relatively large prisms, (I), and tiny needles, (II).

As the enantiopure material was indeed present in the batch and after resolution of the crude mixture at 22% ee by chiral high-pressure liquid chromatography, we tried to grow crystals from one of these pure fractions (Mekki *et al.*, 2011). Unfortunately, this enantiomeric pure fraction crystallizes in the form of needles of even smaller size than those of polymorph (II). These crystals do not give any appreciable diffraction intensity even at long exposure times so it should be concluded that it is apparently very difficult to grow crystals of sufficient size of the enantiopure material. Powder diffraction may be able to confirm the molecular structure of the enantiopure material, but unfortunately this will not give more information about the absolute configuration of the main enantiomer.

### Compound (I)

#### Crystal data

$C_{32}H_{31}NO_7S$	$\gamma = 81.354 (4)^\circ$
$M_r = 573.64$	$V = 1421.06 (12) \text{ \AA}^3$
Triclinic, $P\bar{1}$	$Z = 2$
$a = 10.8577 (4) \text{ \AA}$	Cu $K\alpha$ radiation
$b = 11.1342 (6) \text{ \AA}$	$\mu = 1.43 \text{ mm}^{-1}$
$c = 12.3719 (6) \text{ \AA}$	$T = 173 \text{ K}$
$\alpha = 87.928 (4)^\circ$	$0.40 \times 0.29 \times 0.23 \text{ mm}$
$\beta = 73.958 (4)^\circ$	

#### Data collection

Agilent Xcalibur Sapphire3 Gemini diffractometer	43929 measured reflections
Absorption correction: multi-scan (CrysAlis PRO; Agilent, 2010)	5160 independent reflections
$T_{\min} = 0.589$ , $T_{\max} = 1.000$	4541 reflections with $I > 2\sigma(I)$
	$R_{\text{int}} = 0.072$

#### Refinement

$R[F^2 > 2\sigma(F^2)] = 0.050$	371 parameters
$wR(F^2) = 0.165$	H-atom parameters constrained
$S = 1.18$	$\Delta\rho_{\text{max}} = 0.38 \text{ e \AA}^{-3}$
5160 reflections	$\Delta\rho_{\text{min}} = -0.86 \text{ e \AA}^{-3}$

### Compound (II)

#### Crystal data

$C_{32}H_{31}NO_7S$	$V = 2878.68 (17) \text{ \AA}^3$
$M_r = 573.64$	$Z = 4$
Monoclinic, $P2_1/c$	Cu $K\alpha$ radiation
$a = 10.8712 (4) \text{ \AA}$	$\mu = 1.41 \text{ mm}^{-1}$
$b = 19.8539 (6) \text{ \AA}$	$T = 173 \text{ K}$
$c = 13.8180 (4) \text{ \AA}$	$0.21 \times 0.02 \times 0.02 \text{ mm}$
$\beta = 105.156 (3)^\circ$	

#### Data collection

Agilent Xcalibur Sapphire3 Gemini diffractometer	5477 measured reflections
Absorption correction: multi-scan (CrysAlis PRO; Agilent, 2010)	5477 independent reflections
$T_{\min} = 0.897$ , $T_{\max} = 1.000$	2878 reflections with $I > 2\sigma(I)$
	$R_{\text{int}} = 0.049$
	$\theta_{\text{max}} = 51.8^\circ$

**Table 1**

Selected geometric parameters ( $\text{\AA}$ ,  $^\circ$ ) for (I).

N1—C2	1.458 (3)	C3—C4	1.530 (3)
C2—C1	1.529 (3)	C3—C5	1.548 (3)
C2—C3	1.569 (3)		
S1—N1—H1—C2	157.7		

**Table 2**

Hydrogen-bond geometry ( $\text{\AA}$ ,  $^\circ$ ) for (I).

$D-H\cdots A$	$D-H$	$H\cdots A$	$D\cdots A$	$D-H\cdots A$
O3—H3 $\cdots$ O7 <sup>1</sup>	0.82	2.17	2.914 (2)	152
N1—H1 $\cdots$ O4 <sup>1</sup>	0.88	2.11	2.910 (2)	151

Symmetry code: (i)  $-x, -y + 2, -z$ .

**Table 3**

Selected geometric parameters ( $\text{\AA}$ ,  $^\circ$ ) for (II).

N1—C2	1.461 (8)	C3—C4	1.536 (7)
C2—C1	1.523 (7)	C3—C5	1.546 (7)
C2—C3	1.552 (6)		
S1—N1—H1—C2	-153.0		

**Table 4**

Hydrogen-bond geometry ( $\text{\AA}$ ,  $^\circ$ ) for (II).

$D-H\cdots A$	$D-H$	$H\cdots A$	$D\cdots A$	$D-H\cdots A$
O3—H3 $\cdots$ O7 <sup>1</sup>	0.82	2.30	2.868 (5)	127
N1—H1 $\cdots$ O4 <sup>1</sup>	0.88	2.05	2.920 (5)	169

Symmetry code: (i)  $-x, -y, -z + 1$ .

#### Refinement

$R[F^2 > 2\sigma(F^2)] = 0.067$	370 parameters
$wR(F^2) = 0.234$	H-atom parameters constrained
$S = 0.92$	$\Delta\rho_{\text{max}} = 0.79 \text{ e \AA}^{-3}$
5477 reflections	$\Delta\rho_{\text{min}} = -0.40 \text{ e \AA}^{-3}$

All N- and O-bound H atoms were located in difference Fourier maps but were subsequently included as riding atoms [O—H = 0.82  $\text{\AA}$  and  $U_{\text{iso}}(\text{H}) = 1.5U_{\text{eq}}(\text{O})$ ; N—H = 0.86  $\text{\AA}$  and  $U_{\text{iso}}(\text{H}) = 1.2U_{\text{eq}}(\text{N})$ ] in order to stabilize their coordinates during the final step of the refinement. All other H atoms were introduced at calculated positions and refined as riding atoms, with C—H = 0.96–0.98  $\text{\AA}$  and  $U_{\text{iso}}(\text{H}) = 1.5U_{\text{eq}}(\text{C})$  for methyl and  $1.2U_{\text{eq}}(\text{C})$  for all other H atoms. Polymorph (II) was found to be twinned by reticular merohedry with a twin index 3. The twin symmetry element is a twofold axis along the reciprocal  $c$  axis and the pseudo-orthorhombic lattice can be generated by  $a' = a$ ,  $c' = 3c - a'$ ,  $c' = c$ . A merged HKLF5-type file was used for the refinements. The twin fractions were found to be 0.854 (1) and 0.146 (1). Accounting for the twinning resulted in slightly lower s.u. values on refined parameters.

For both compounds, data collection: *CrysAlis PRO* (Agilent, 2010); cell refinement: *CrysAlis PRO*; data reduction: *CrysAlis PRO*; program(s) used to solve structure: *SHELXS97* (Sheldrick, 2008); program(s) used to refine structure: *SHELXL97* (Sheldrick, 2008); molecular graphics: *OLEX2* (Dolomanov *et al.*, 2009); software used to prepare material for publication: *PLATON* (Spek, 2009) and *pubCIF* (Westrip, 2010).

This work was supported by the Erasmus Mundus Averroés programme.

Supplementary data for this paper are available from the IUCr electronic archives (Reference: GZ3195). Services for accessing these data are described at the back of the journal.

## References

- Agilent (2010). *CrysAlis PRO*. Agilent Technologies, Yarnton, Oxfordshire, England.
- Allen, F. H. (2002). *Acta Cryst.* **B58**, 380–388.
- Bernstein, J. (2002). *Polymorphism in Molecular Crystals*. IUCr Monographs on Crystallography, No. 14. New York: Oxford University Press Inc.
- Bernstein, J. (2011). *Cryst. Growth Des.* **11**, 623–650.
- Bernstein, J., Davis, R. E., Shimoni, L. & Chang, N. L. (1995). *Angew. Chem. Int. Ed. Engl.* **34**, 1555–1573.
- Chisholm, J. A. & Motherwell, S. (2005). *J. Appl. Cryst.* **38**, 228–231.
- Danbolt, N. C. (2001). *Prog. Neurobiol.* **65**, 1–105.
- Dolomanov, O. V., Bourhis, L. J., Gildea, R. J., Howard, J. A. K. & Puschmann, H. (2009). *J. Appl. Cryst.* **42**, 339–341.
- Dunitz, J. D. (1979). *X-ray Analysis and the Structure of Organic Molecules*. Ithaca, NY: Cornell University Press.
- Esslinger, C. S., Agarwal, S., Gerdes, J., Wilson, P. A., Davis, E. S., Awes, A. N., O'Brien, E., Mavencamp, T., Koch, H. P., Poulsen, D. J., Rhoderick, J. F., Chamberlin, A. R., Kavanaugh, M. P. & Bridges, R. J. (2005). *Neuropharmacology*, **49**, 850–861.
- Gavezzotti, A. (1994). *Acc. Chem. Res.* **27**, 309–314.
- Gavezzotti, A. & Filippini, G. (1994). *J. Phys. Chem.* **98**, 4831–4837.
- Glusker, J. P. (1994). *Crystal Structure Analysis for Chemists and Biologists*, edited by A. P. Marchand, pp. 321–323. New York: VCH Publishers Inc.
- Jones, N. A., Jenkinson, S. F., Soengas, R., Izumori, K., Fleet, G. W. J. & Watkin, D. J. (2007). *Acta Cryst.* **C63**, o7–o10.
- Li, G., Chang, H. T. & Sharpless, K. B. (1996). *Angew. Chem. Int. Ed. Engl.* **35**, 451–454.
- Macrae, C. F., Edgington, P. R., McCabe, P., Pidcock, E., Shields, G. P., Taylor, R., Towler, M. & van de Streek, J. (2006). *J. Appl. Cryst.* **39**, 453–457.
- Maragakis, N. J. & Rothstein, J. D. (2004). *Neurobiol. Dis.* **15**, 461–473.
- Mekki, S., Bellahouel, S., Vanthuynne, N., Rolland, M., Derdour, A., Martinez, J. & Rolland, V. (2011). *Amino Acids*. Submitted.
- Mitscherlich, E. (1822). *Ann. Chim. Phys.* **19**, 350–419.
- Sheldrick, G. M. (2008). *Acta Cryst.* **A64**, 112–122.
- Shimamoto, K., Shigeri, Y., Yasuda-Kamatani, Y., Lebrun, B., Yumoto, N. & Nakajima, T. (2000). *Bioorg. Med. Chem. Lett.* **10**, 2407–2410.
- Spek, A. L. (2009). *Acta Cryst.* **D65**, 148–155.
- Streuff, J., Nieger, M. & Muñiz, K. (2006). *Chem. Eur. J.* **12**, 4362–4371.
- Streuff, J., Osterath, B., Nieger, M. & Muñiz, K. (2005). *Tetrahedron Asymmetry*, **16**, 3492–3496.
- Westrip, S. P. (2010). *J. Appl. Cryst.* **43**, 920–925.
- Zhao, Y., Jiang, N., Chen, S., Peng, C., Zhang, X., Zou, Y., Zhang, S. & Wang, J. (2005). *Tetrahedron*, **61**, 6546–6552.